ZnO film thickness effect on surface acoustic wave modes and acoustic streaming

X. Y. Du,[1] Y. Q. Fu,[1] S. C. Tan,[1] J. K. Luo,[1,a)] A. J. Flewitt,[1] W. I. Milne,[1] D. S. Lee,[2] N. M. Park,[2] J. Park,[2] Y. J. Choi,[2] S. H. Kim,[2] and S. Maeng[2]
[1]*Centre for Advanced Photonics and Electronics, Department of Engineering, University of Cambridge, 9 JJ Thomson Ave, CB3 0FA, United Kingdom*
[2]*Electronics and Telecommunications Research institute (ETRI), 161 Gajeong-dong, Yuseong-gu, Daejeon 305-700, Republic of Korea*

(Received 9 July 2008; accepted 24 July 2008; published online 4 September 2008)

Surface acoustic wave (SAW) devices were fabricated on ZnO thin films deposited on Si substrates. Effects of ZnO film thickness on the wave mode and resonant frequency of the SAWs have been investigated. Rayleigh and Sezawa waves were detected, and their resonant frequencies decrease with increase in film thickness. The Sezawa wave has much higher acoustic velocity and larger signal amplitude than those of Rayleigh mode wave. Acoustic streaming for mixing has been realized in piezoelectric thin film SAWs. The Sezawa wave has a much better efficiency in streaming, and thus is very promising for application in microfluidics. © *2008 American Institute of Physics*. [DOI: 10.1063/1.2970960]

Microfluidics is very important for life science, drug development, and healthcare. Mixing liquids of a few picoliters to a few microliters is an extremely delicate task as it is dominated by the interaction between the fluid and surface of the substrate when the surface to volume ratio becomes large in microdimensions. Currently micromixing is dominated by passive mixing using static structures such as microposts and serpentine channels. However, efficient mixing of liquids in passive mixers is found to be difficult.[1,2]

The surface acoustic wave (SAW) has recently found extraordinary applications in microfluidics and laboratory-on-a-chip.[3–9] When the propagating acoustic wave meets the liquid on its path, its energy and momentum are coupled into the liquid, inducing acoustic streaming and droplet motion, which can be used for pumping and mixing liquids.[3–9] SAW-based microfluidics offer the advantages of simple device structure with no moving parts, high reliability, and low cost. SAW can be used as biochemical sensors with high sensitivity.[10] Sensors and microfluidics are the two main components for laboratory-on-a-chip.

The technologies, however, have only been realized using bulk piezoelectric (PE) materials, such as quartz or $LiNbO_3$,[3–9] which cannot be integrated with Si-based integrated circuits (IC). PE thin films, such as AlN and ZnO, have been developed to fabricate SAWs used in electronics and rf communications,[10,11] but are not common in microfluidics and sensors. Thin film SAWs possess several advantages, such as low power consumption, low cost, and the possibility of integration with IC control circuits. In this study, a ZnO thin film is selected as the PE material to fabricate SAW microfluidics.

For thin film SAWs, a high-order (HO) harmonic wave is typically too weak to exist. However there exist HO Sezawa (S)-mode waves in SAWs with layered structures in which the substrate has a higher acoustic velocity than the overlaying film.[14,15] The appearance of the S-mode waves is determined by the ratio of the PE film thickness h to the wavelength λ. By varying the thickness of the PE film, the phase velocity of the acoustic wave can be varied between the acoustic velocities of the surface PE layer and the substrate material. It is necessary to clarify how the ZnO film thickness affects the resonant frequencies and streaming velocity before application for microfluidics.

ZnO films with different thicknesses (from 0.15 to 6.6 μm) were deposited on Si (100) using rf magnetron sputtering from a Zn target at a power of 200 W and Ar/O_2 (30SCCM/10SCCM) mixture gas (SCCM: denote standard cubic centimetre per minute).[12] The morphology, crystallinity and stoichiometry of the films were charaterised by scanning electron microscopy (SEM), x-ray diffraction (XRD) and x-ray photoelectron spectroscopy (XPS) respectively.

The aluminum interdigited transducer (IDT) electrodes were fabricated using a sputtering and lift-off process on top of the ZnO film. The Al thickness is ~150 nm. The IDTs consist of 30 and 60 pairs of fingers, with an aperture of 4900 μm and a spatial periodicity of 32 μm. An HP8711A rf network analyzer was used to measure the resonant frequency and signal amplitude of the SAW devices.

SEM characterization showed that ZnO films have a columnar grain structure perpendicular to the surface as ZnO crystals typically grow as long hexagonal rods along the c-axis.[13] C-axis ZnO structures are preferential structures for SAWs used for microfluidics, which normally require a wave displacement perpendicular to the surface [Rayleigh (R)-mode wave]. XPS analysis showed that the ZnO films are stoichiometric for all the deposited films. XRD spectra of different thickness ZnO films showed a single peak close to 34.2° that corresponds to the diffraction from the (002) plane of the ZnO. Crystallite sizes calculated from the Debye–Scherrer formula[14] increase from 14 to 28 nm as the film thickness increases from 0.15 to 6.6 μm.

Figure 1 shows the reflection signals of the SAWs with different ZnO thickness. With a ZnO thickness below 1.0 μm ($hk<0.3$, $k=2\pi/\lambda$: wave vector), no wave mode could be detected due to the low electromechanical coupling

a)Author to whom correspondence should be addressed. Electronic mail: jl2@bolton.ac.uk. Present address: University of Bolton.

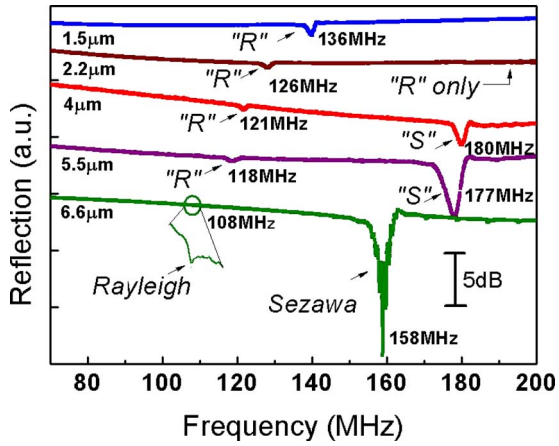

FIG. 1. (Color online) Reflection spectra of SAWs with ZnO thickness as a parameter. The resonant frequency of both Rayleigh and Sezawa waves decrease as the thickness increases. The amplitudes of Sezawa waves are much larger than those of Rayleigh wave.

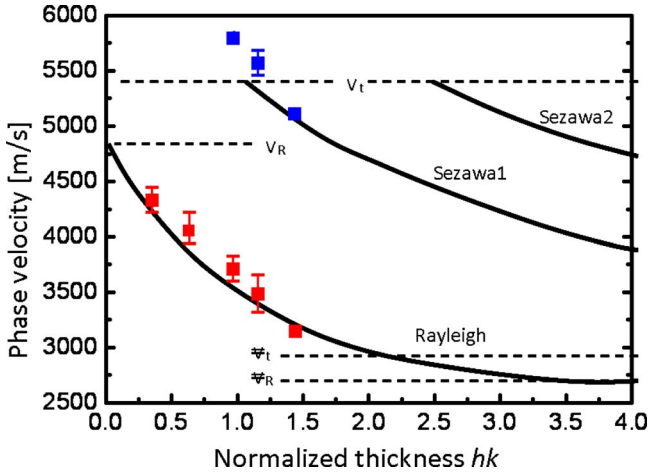

FIG. 2. (Color online) Dependence of phase velocities for the Rayleigh and Sezawa mode waves on normalized thickness of ZnO film, hk. Here V_R and $\mathbb{V}_R$ are the Rayleigh velocities, and V_t, and $\mathbb{V}_t$ are the shear velocities of the Si substrate and ZnO film (Ref. 13).

for a very thin ZnO film using a wavelength of 32 μm.[15,16] For devices with ZnO thickness between 1.5 and 2.8 μm, the R-mode resonant peak starts to appear, and the reflection signal becomes stronger in SAWs with thicker ZnO films. The resonant frequency gradually decreases with increasing ZnO thickness. The variation in the phase velocity of the R-mode wave with the film thickness can be explained from the penetration depth of the R-wave into the substrate. For a thinner film, the acoustic wave can penetrate relatively deeper into the substrate[17] and most of the SAW energy is localized in the substrate. The phase velocity of the SAW approaches the Rayleigh velocity of the substrate material, the Si here. The velocity of the SAW propagating in the Si (4680 m/s) is higher than that in ZnO (2700 m/s).[18] With the increase in the ZnO layer thickness, more acoustic energy localizes within the ZnO, thus the acoustic wave velocity gradually decreases and reaches that of the ZnO film. Results in Fig. 1 clearly show that the resonant frequency of the R-wave decreases from 136 to 108 MHz as the thickness increases from 1.5 to 6.6 μm (the hk changes from 0.3 to 1.3), corresponding to a decrease of the acoustic velocity from 4352 to 3456 m/s. Theoretical analysis showed that the phase velocity is close to that of the Rayleigh velocity of the substrate at $hk \sim 0$, and deceases monotonically until it approaches the Rayleigh velocity of the surface material at $hk \gg 1$.[18] Figure 2 provides a comparison between the measured phase velocity and the theoretical analysis for the R-wave and shows good agreement.

No HO harmonic Rayleigh wave was observed from the above ZnO SAWs. With the ZnO thickness larger than 2.8 μm, a HO resonant peak, the Sezawa wave, appears in addition to the R-wave, as shown in Fig. 1. The S-wave exhibits a higher phase velocity (higher resonant frequency) than the R-wave for a fixed thickness. The amplitude of the S-wave was found to be much larger than that of the R-wave, typically five to ten times that of the R-wave, and it increases with the ZnO film thickness. This is attributed to the improved film quality, PE property. and electromechanical coupling coefficient in a thick film. Similar to that of R-wave, the resonant frequency, hence the phase velocity of the S-wave decreases with film thickness as it is gradually dominated by the substrate acoustic velocity.

Higher frequency S-waves are induced at a certain thickness approximately $hk=1$ for the first Sezawa mode.[18] The first mode S-waves were observed from SAWs with ZnO of 4–6.6 μm (corresponding to $hk=0.8-1.3$), consistent with the theoretical analysis. The appearance of the S-wave in a device with $hk<1$ implies improved crystalinity as only those with high crystal quality and large electromechanical coupling coefficient can produce S-wave in a device with $hk<1$.[18] The measured velocity of the S-wave and the theoretical one are once again in good agreement, as shown in Fig. 2.

Water droplets with a volume of ~ 10 μl were loaded on the surface of the SAWs. The ZnO surface is hydrophilic, but it is extremely sensitive to the light exposure.[19] The samples were cleaned before each measurement, and the water contact angle on these ZnO surfaces remains relatively constant at 75°–81°. An ac signal of the resonant frequency from an Agilent N9310A signal generator was amplified by a power amplifier and applied to the IDT. The streaming velocity was determined by measuring the speed of the black ink particles added in the liquid moving through the center of the droplet using a digital camera (MOTICAM2000) with built-in software for analysis.

As the voltage increases to a certain level, acoustic streaming was observed with a semicircle flow pattern, as shown in Fig. 3(a). Increasing the signal voltage enhances the streaming velocity. It was observed that both the R- and S-waves can induce acoustic streaming with different velocity, as shown in Fig. 3(b). The streaming velocity induced by the S-wave is much higher than that by the R-wave. Figure 4 shows the dependence of the streaming velocity on an ac voltage as a function of IDT pair numbers and wave modes. The streaming velocity increases linearly with increase in voltage, and the velocity increases with the film thickness at a fixed signal voltage. These are attributed to the increased transmission signal as the ZnO thickness increase. For the same devices, the streaming velocity induced by the S-wave is typically three to five times higher than that by R-wave owing to the large transmission amplitude. The results clearly show that the S-waves have a high resonant frequency and high signal amplitude and as such it is more suitable for high frequency sensor and microfluidic system applications.

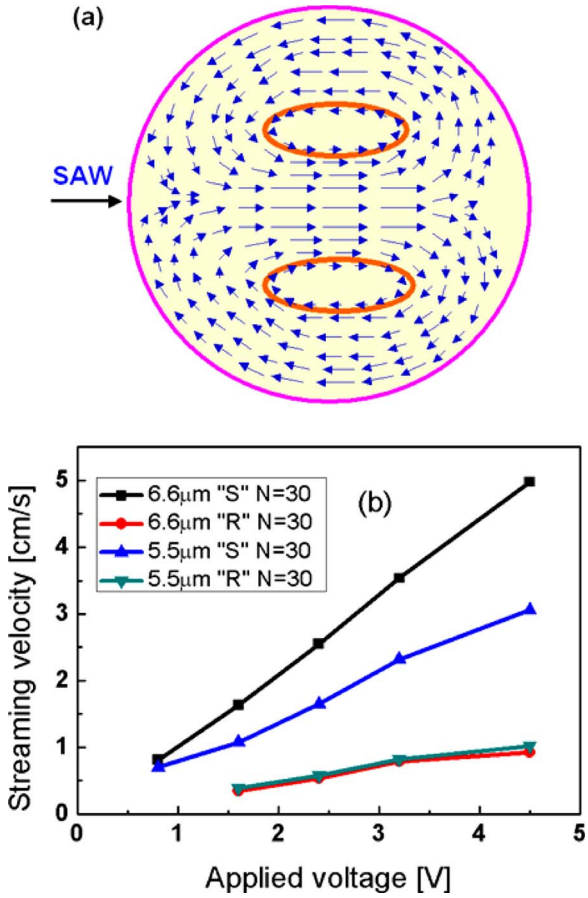

FIG. 3. (Color online) (a) The acoustic streaming pattern within a droplet and (b) comparison of streaming velocities induced by Rayleigh and Sezawa mode waves. Sezawa wave generates much high streaming velocity than that by Rayleigh wave.

The amplitude of the resonant wave can also be enhanced by using more IDT fingers N. Results in Fig. 4 for SAWs with finger pairs of $N=30$ and 60 clearly show the increased streaming velocity in SAWs with 60 pair of fingers. According to the crossed-field model, the radiation conductance $G_a(f_o)$ of an acoustic wave at the resonant frequency f_o, can be expressed as[20,21]

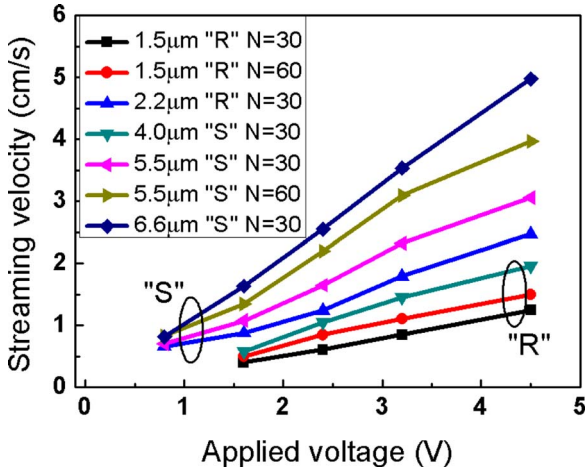

FIG. 4. (Color online) Streaming velocity as a function of ac signal voltage with IDT finger pair and wave mode as a parameter. "S" and "R" stand for Sezawa and Rayleigh mode waves, respectively.

$$G_a(f_o) = 8K^2 f_o CN, \tag{1}$$

where C is the input capacitance and K^2 the electromechanical coupling coefficient. The radiation conductance is high for a SAW with high resonant frequency and large finger pairs (which is also associated with large C). This, in turn, increases the mechanical energy at a fixed input signal. The Sezawa mode also possesses a higher $K^2 \sim 4\%$,[22] compared with $K^2 \sim 0.49\%$ for the R-wave,[23] implying the S-wave is better for microfluidic applications.

In summary, the acoustic velocity of a thin ZnO SAW is close to that of the Si substrate, decreases with the ZnO thickness, and approaches that of the bulk ZnO as the thickness increases. A Sezawa mode wave with a higher resonant frequency was observed from devices with a ZnO film >2.8 μm. The signal amplitude of the S-wave is much stronger than that of the R-wave. Acoustic streaming was realized for the first time on the ZnO SAWs using both the R- and S-waves. However, the S-wave induces much stronger streaming than that produced by the R-wave; hence, it is more suitable for thin-film SAW microfluidics.

This work was supported by the IT R&D program of MIC/IITA, Republic of Korea (2005-S605-02, IT-BT-NT Convergent Core Technology for advanced Optoelectronic Devices and Smart Bio/Chemical Sensors).

[1] X. Chen, D. F. Cui, C. C. Liu, H. Li, and J. Chen, Anal. Chim. Acta **584**, 237 (2007).
[2] Z. M. Wu and D. Q. Li, Electrochim. Acta **53**, 5827 (2008).
[3] A. Toegl, J. Scriba, A. Wixforth, C. Strobl, C. Gauer, and Z. V. Guttenberg, Anal. Bioanal. Chem. **379**, 982 (2004).
[4] K. Chono, N. Shimizu, Y. Matsui, J. Kondon, and S. Shiokawa, Jpn. J. Appl. Phys., Part 1 **43**, 2987 (2004).
[5] S. Alzuaga, S. Ballandras, F. Daniau, W. Gauthier, B. Manceau, and R. Duhamel, Proc.-IEEE Ultrason. Symp. **2**, 1790 (2003).
[6] A. Renaudin, P. Tabourier, V. Zhang, J. C. Camart, and C. Druon, Sens. Actuators B **113**, 389 (2006).
[7] K. Lange, G. Blaess, A. Voigt, R. Gotzen, and M. Rapp, Biosens. Bioelectron. **22**, 227 (2006).
[8] H. Li, J. Friend, and L. Yeo, Biomed. Microdevices **28**, 4098 (2007).
[9] R. Shilton, M. K. Tan, L. y. Yeo, and J. R. Friend, J. Appl. Phys. **104**, 014910 (2008).
[10] T. M. Gronewold, Anal. Chim. Acta **603**, 119 (2007).
[11] N. W. Emanetoglu, C. Gorla, Y. Liu, S. Liang, and Y. Lu, Mater. Sci. Semicond. Process. **2**, 247 (1999).
[12] J. Shilton, V. Talyanskii, M. Pepper, D. Ritchie, J. Frost, C. Ford, C. Smith, and G. Jones, J. Phys.: Condens. Matter **8**, L531 (1996).
[13] K. B. Sundaram and A. Khan, Thin Solid Films **295**, 87 (1997).
[14] W. L. Dang, Y. Q. Fu, J. K. Luo, A. J. Flewitt, and W. I. Milne, Superlattices Microstruct. **42**, 89 (2007).
[15] T. Wu and W. Wang, J. Appl. Phys. **96**, 9 (2004).
[16] S. Wu, Y. Chen, and T. Chang, Jpn. J. Appl. Phys., Part 1 **41**, 4605 (2002).
[17] A. Talbi, F. Sarry, L. Brizoual, O. Elmazriza, and P. Alnot, IEEE Trans. Ultrason. Ferroelectr. Freq. Control **51**, 1421 (2004).
[18] V. Panella, G. Carlotti, G. Socino, L. GioVannini, M. Eddrief, K. Amimer, and C. Sebenne, J. Phys.: Condens. Matter **9**, 5575 (1997).
[19] G. Kenanakis, E. Stratakis, K. Vlachou, D. Vernardou, E. Koudoumas, and N. Natsarakis, Appl. Surf. Sci. **254**, 5695 (2008).
[20] D. Powell, K. Kalantar, and W. Wlodarki, Sens. Actuators, A **115**, 456 (2004).
[21] C. K. Campell, *SAW for Mobile and Wireless Communications* (Academic, San Diego, 1998).
[22] I. Tang, H. Chen, M. Houng, and Y. Wang, Solid-State Electron. **47**, 2063 (2003).
[23] L. Brizoual, O. Elmazria, F. Sarry, and M. Hakiki, Ultrasonics **45**, 100 (2006).